

# Diverging Cusped-Field Hall Thruster (DCHT)

IEPC-2007-39

*Presented at the 30<sup>th</sup> International Electric Propulsion Conference, Florence, Italy  
September 17-20, 2007*

Daniel G. Courtney\* and Manuel Martínez-Sánchez†

*Massachusetts Institute of Technology, Cambridge, Massachusetts, 02139*

An experimental cusped field Hall thruster has been developed as a test bed for exploring its viability as an alternative to more traditional magnetic arrangements in Hall thrusters. Design details and preliminary test results of the Diverging Cusped-field Hall Thruster (DCHT) are presented. The thruster design features strong magnetic cusps arranged in a divergent formation and follows from studies performed by both THALES Electron Devices and the Princeton University Plasma Propulsion Laboratory (PPL). Visual observations and current measurements of preliminary voltage scans performed at the MIT Space Propulsion Laboratory (SPL) are presented. Furthermore, thrust data collected at the Busek Company in Natick, Massachusetts are discussed. Throughout all trials the DCHT operated at power levels between 102 and 538W. A peak efficiency of 44.5% was recorded at a flow rate of 8.5sccm and 550 Volts applied to the anode. Here, the thrust measured 13.4mN and the specific impulse was 1641s. Preliminary observations of deposition profiles on the thruster walls are discussed.

## Nomenclature

$e$	= electron charge
$I_a$	= anode current
$I_{sp}$	= anode specific impulse
$g$	= acceleration due to gravity
$\dot{m}_a$	= anode flow rate
$P_a$	= anode power
$T$	= thrust
$\eta_t$	= anode thrust efficiency

## I. Introduction

HALL thrusters have emerged as a viable option for station keeping and control of satellites in Earth orbit. Since their inception they have been the subject of both detailed experimental work and thorough simulations. However; until recently, the basic magnetic configuration has remained relatively static. Within the past decade several groups<sup>1,2</sup> have looked at making changes to the magnetic arrangement by using cusped field structures in order to improve the overall performance of Hall thrusters. Specifically, the Cylindrical Hall Thruster (CHT) developed at the Princeton University Plasma Propulsion Laboratory (PPL)<sup>1</sup> and the High Efficiency Multi-stage Plasma (HEMP) thrusters designed<sup>3,4</sup> and patented<sup>5</sup> by THALES Electron Devices have both employed cusped fields. In addition, cusped fields similar to the arrangement presented here have long been employed in ion thrusters<sup>6</sup> as an effective means of controlling electron mobility.

The goal of the MIT Diverging Cusped-field Hall Thruster (DCHT) project is to gain a better understanding of the characteristics of cusped field thrusters and to evaluate the future potential of the concept through analysis of an experimental device. At this stage, our primary motivation for using cusped fields is not a

---

\*Graduate Student, Department of Aeronautics and Astronautics, dcourt@mit.edu

†Professor, Department of Aeronautics and Astronautics, mmart@mit.edu.

dramatic shift in performance but rather increased life through protecting the thruster components. Cusped field structures introduce strong magnetic bottles which provide the ability to localize the discharge plasma through repulsive forces which result from steep magnetic gradients. Since the electron guiding centers are repelled magnetically from the walls, the sheath potential required to balance electron and ion currents to the walls will be lowered. This in turn decreases the energy of ions accelerated through the sheath towards the channel walls.<sup>4</sup> Furthermore, the presence of a cusped field in the approach to anode surfaces has been shown to impede electrons and enhance ionization efficiencies.<sup>6</sup> Finally, cusped field arrangements allow for high magnetic field strengths using relatively small permanent magnets. This suggests that, if properly understood, cusped field thrusters could be well suited for miniature Hall type thrusters where high strength magnetic fields are desirable.<sup>7</sup>

## II. The Diverging Cusped-field Hall Thruster Overview

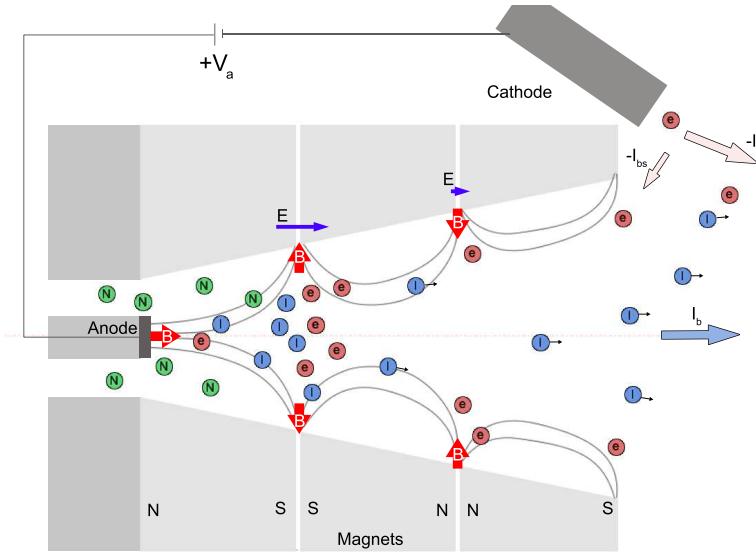


Figure 1. Schematic diagram of the DCHT basic operating principles.

The DCHT is schematically illustrated in Fig. 1. Three permanent magnets are arranged in a divergent pattern resulting in two distinct cusps within the channel and a strong magnetic bottling near the anode. We hope that these cusps will produce sufficient magnetic gradients to protect both the anode and discharge chamber surfaces, leading to longer life performance.

Despite the irregular magnetic field profiles within the DCHT, the basic process for producing thrust remains identical to that of traditional Hall thrusters. Electron guiding centers are confined, at some location, to closed drifts resulting primarily from  $\vec{E} \times \vec{B}$  effects. With the electrons confined to these drifts a potential gradient develops between them and the anode potential. Ions are then electrostatically accelerated by the resultant electric field. Finally, thrust is conveyed to the body by magnetic forces between the confined electrons and the magnets themselves.

The DCHT design is primarily based on the experience gained from the THALES HEMP cylindrical thrusters<sup>3</sup> and the Princeton CHT.<sup>1</sup> Specifically, as in the HEMP thrusters, we expect to localize electrons in closed orbits near the first cusp where the  $\vec{B}$  fields are mostly radial. As a result, we anticipate both ionization and acceleration of ions to be strongly localized in this area. This is in contrast to the CHT where ionization is reported to occur in the coaxial region at the base of the thruster and ion acceleration in the cylindrical region between the anode and cusp.<sup>1</sup> The third magnet and divergent channel shape have been included for several reasons. First, similar to the CHT,<sup>1</sup> the increased area downstream of the ionization and acceleration regions should reduce ion losses to the walls. Secondly, the additional cusp provides a further reduction in electron mobility towards the anode by completing a magnetic mirror between itself and the upstream cusp. In addition, given the high field strengths within the thruster shown in Fig. 3(b)

ions may become weakly magnetized as they pass through the discharge channel. At field strengths of up to 0.5T, an ion accelerated through anode potentials up to 600V could have a Larmor radius on the order of 60mm, which is comparable to the thruster dimensions. The divergent shape of the magnets reduces the magnetic field strength exposed to axially accelerated ions as they progress from the first cusp towards the exit plane. This additional motivation, stems from the tendency of cusped field thrusters to feature strong highly divergent fields at the thruster exit plane. Magnetized ions may be slightly deflected by such fields which would promote beam divergence and thereby reduce performance.

### III. DCHT Design Features

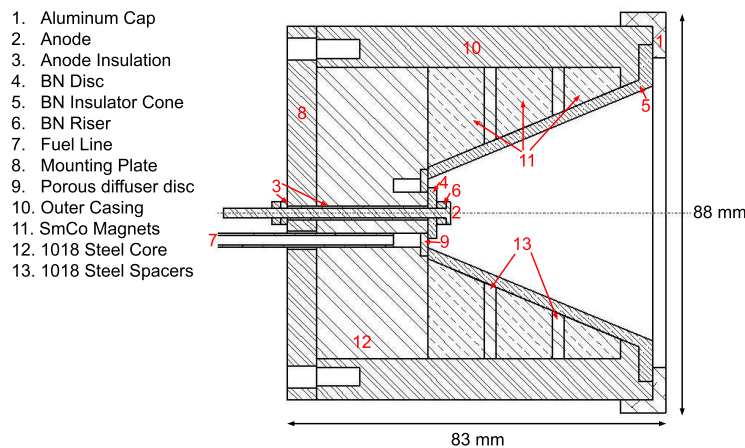


Figure 2. Cross-section view of the DCHT components.

Details of the magnetic arrangement used to create the field along with important aspects of the overall design are discussed in this section. A scaled engineering drawing of the thruster is presented in Fig. 2 and a picture of the completed assembly in Fig. 4.

#### A. Magnetic Circuit Design

The magnetic circuit was designed using the Ansoft Maxwell software package. The resultant field shown in Fig. 3 is produced by three permanent magnets. Two strong cusps, with primarily radial fields between the magnets are visible in Fig. 3(a). The maximum field strength in Fig. 3(b) is approximately 0.5T and occurs at the first(upstream) cusp. Samarium Cobalt (SmCo) permanent magnets were selected to satisfy the requirements of both high field strength and good thermal behavior. Specifically, custom SmCo 3212 magnets featuring a divergent feature were prepared by Dexter Magnetic Technologies. These magnets have a manufacturer rated maximum operating temperature of 300°C and a Currie temperature of 825°C.<sup>8</sup>

#### B. Anode and Fuel Inlet

The propellant feed and anode are physically disconnected in the DCHT design, see Fig. 2. This allows for flexibility when optimizing performance by allowing the anode position to be varied independent of the propellant inlet. Figure 3(b) confirms that the anode position, just above the central stem of the core steel base, is in a region of strong magnetic gradients. This serves to protect the anode through a magnetic bottling effect. However, it is conceivable that the electron mobility could be overly restricted by these gradients. The anode is thus allowed to be repositioned using various sizes of boron nitride spacers. During all successful trials reported in this paper, the anode was placed 4 mm from the core stem. The anode is electrically isolated from the thruster body using a sleeve and several washers machined from HP grade boron nitride.

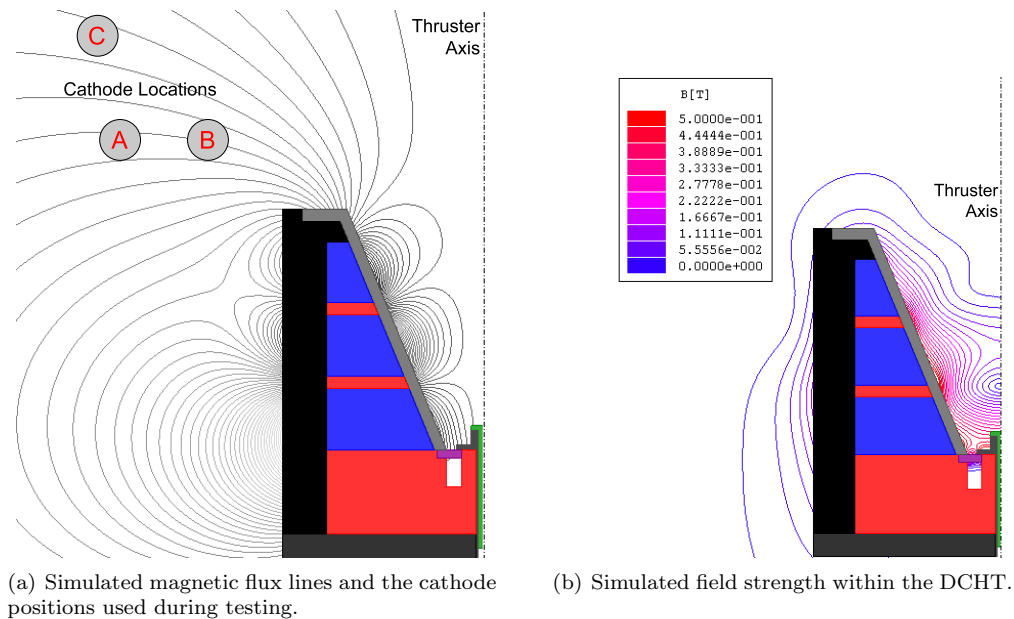


**Figure 3. DCHT magnetic field simulated using Ansoft Maxwell software.**

Propellant is fed through a ring of porous stainless steel inserted at the downstream edge of the annular channel in the base core material, see Fig. 2. The porous ( $10\mu\text{m}$  pore size) stainless steel is intended to effectively stagnate the flow in the annular channel, before allowing propellant to diffuse uniformly through the disc and into the discharge channel.

### C. Dielectric Channel Walls

The dielectric wall of the channel consists of single piece of HP grade boron nitride, turned into a flanged cone by Saint Gobain Ceramics.<sup>9</sup> Boron nitride was selected because it can be easily machined into complex shapes and is frequently used in SPT type Hall thrusters.<sup>10</sup> This heritage will allow more direct comparisons between the erosion characteristics of the DCHT and those of more traditional Hall thrusters.

### D. Cathode Position

During all tests the thruster was equipped with a Busek built hollow cathode shown in Fig.4. A simple cathode mounting system allowed for the position of the cathode to be varied easily. As will be discussed shortly, the cathode position had a significant impact on the thruster operating characteristics. Referring to Fig. 3(a), three cathode locations labeled A, B and C were used. Although the magnetic field strength at the cathode location is far less than that within the discharge channel, it is not insignificant (around  $\sim 0.010\text{T}$  at position B) and may have a strong influence on cathode coupling to the plume.



**Figure 4. Assembled DCHT and Busek hollow cathode prior to initial testing.**

## IV. Experimental Facilities and Performance Metrics

The DCHT was tested at two facilities. Voltage and current measurements along with visual observations were conducted at the MIT Space Propulsion Laboratory (SPL). Further trials, including thrust measurements were performed at the Busek Company in Natick, Massachusetts. For all tests the cathode was current

regulated to operate at 0.25A to the keeper while the required keeper potential was allowed to vary. The thruster body was left at floating potential by means of a dielectric slab placed under the thruster base and by a ceramic break inserted in the propellant line. A virtual ground was created at the cathode potential. The anode, cathode keeper and cathode heater potentials were applied with respect to this point.

The MIT SPL vacuum facility consists of a 1.5m by 1.6m chamber equipped with a mechanical roughing pump and two CTI cryopumps. The pressure did not exceed  $4.2 \times 10^{-5}$ Torr while operating at a maximum flow rate of 10.0sccm. Two 1.0kW Sorensen DC power supplies were used to meet the anode and cathode power requirements.

At Busek, the thruster was tested in tank T6 (measuring 6' in diameter). This tank was equipped with a mechanical pump, a diffusion pump and a cyropump. Pressure did not exceed  $4.4 \times 10^{-5}$ Torr while again operating at a maximum flow rate of 10.0sccm. Here a thrust balance, accurate to within  $\pm 1.6$ mN, was available. The addition of thrust measurements allowed for basic performance evaluations to be made when combined with readings of anode current and potential. The anode thrust efficiency was calculated using the thrust, the anode flow rate and the anode power as in equation 1 below. The average specific impulse was calculated using the thrust and anode flow rate as in equation 2.

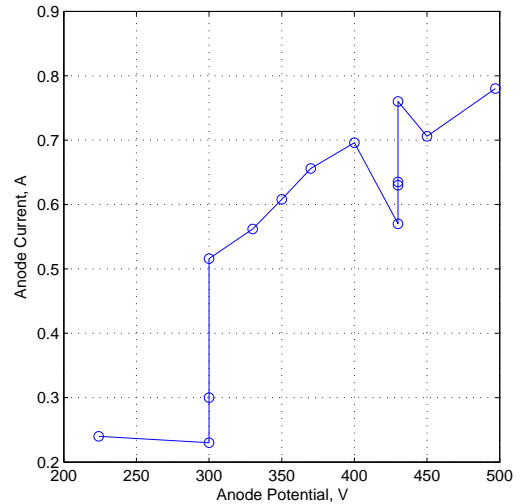
$$\eta_t = \frac{T^2}{2\dot{m}_a P_a} \quad (1)$$

$$I_{sp} = \frac{T}{\dot{m}_a g} \quad (2)$$

## V. Preliminary Test Results and Observations



(a) Visible discharge of the first successful DCHT test.



(b) Measured anode current with increasing anode potential at a constant flow rate of 8.5 sccm.

**Figure 5. First firing of the DCHT, with cathode in position B.**

Numerous tests at both SPL and Busek have yielded preliminary performance data along with some basic observations concerning the impact of cusped fields within the discharge channel.

### A. Preliminary Testing at SPL

During all tests the flow rate was held constant while the applied anode potential was varied. An initial attempt, with the cathode located in position A in Fig. 3(a), did not produce a discharge at anode potentials up to 600V. The cathode was moved to position B and a discharge was produced with 250V to the anode at

a flow rate of 8.5sccm, see Fig. 5(a). A voltage scan was then performed, the anode current measurements are presented in Fig. 5(b)

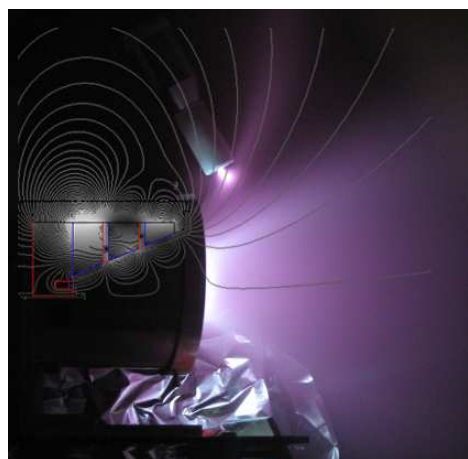


**Figure 6.** Simulated magnetic field overlaid onto the visible plume.

The cathode keeper potential was alarmingly high during the first successful test run, between 70 and 110V. Far greater than the expected value, between 20 and 35V, when the same cathode is operated with commercial Hall thrusters. Fig. 6 shows the simulated magnetic field overlaid onto the plasma discharge. It is apparent from the figure that electrons emitted from the cathode were following magnetic field lines. This suggests that the abnormal keeper behavior may have been caused by magnetic effects.

In an effort to reduce the impact of the magnetic field on the cathode performance and reduce the required keeper potential, the cathode was moved to position C in Fig. 3(a). At this position, the field strength was about half that at position B ( $\sim 0.005\text{T}$ ). Several anode potential scans at various flow rates were performed with the cathode at position C. The resultant current measurements are presented in Fig. 7. During these scans the maximum anode power was 538W, occurring at a flow rate of 10.0sccm with 600V applied to the anode.

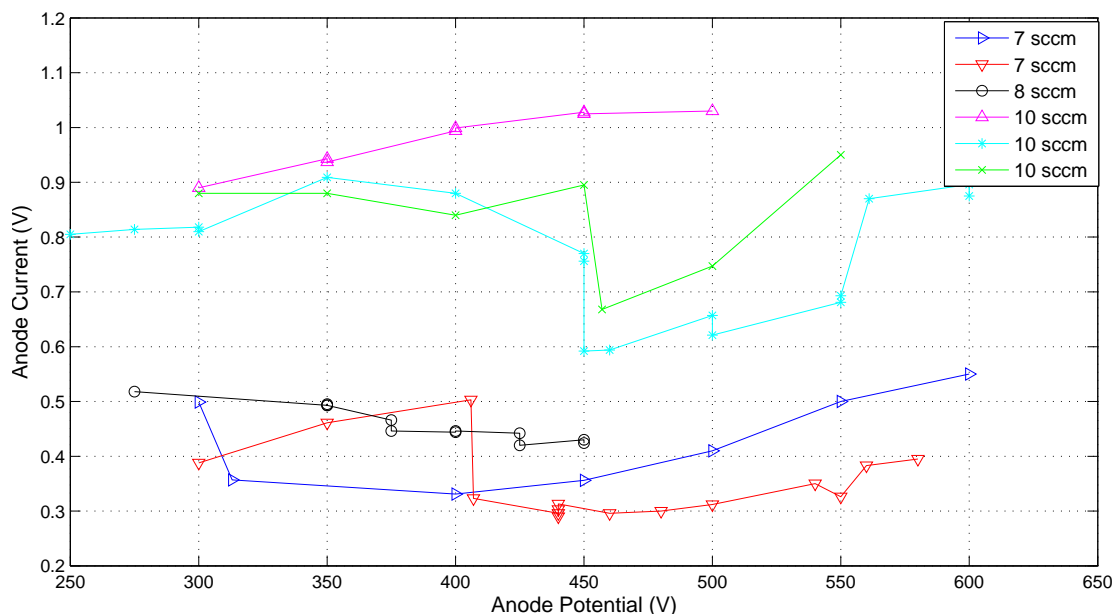
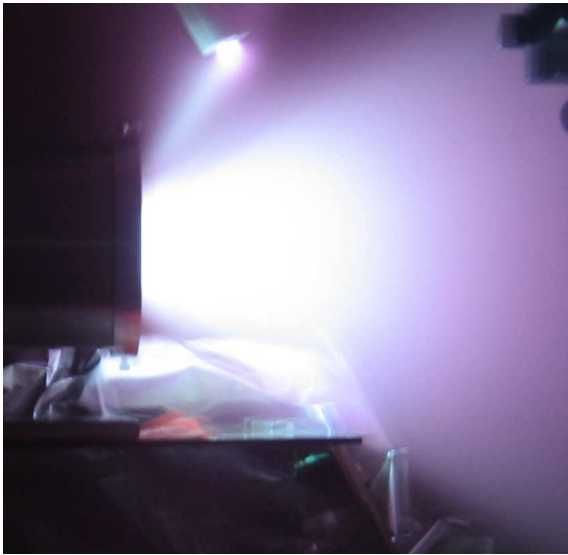


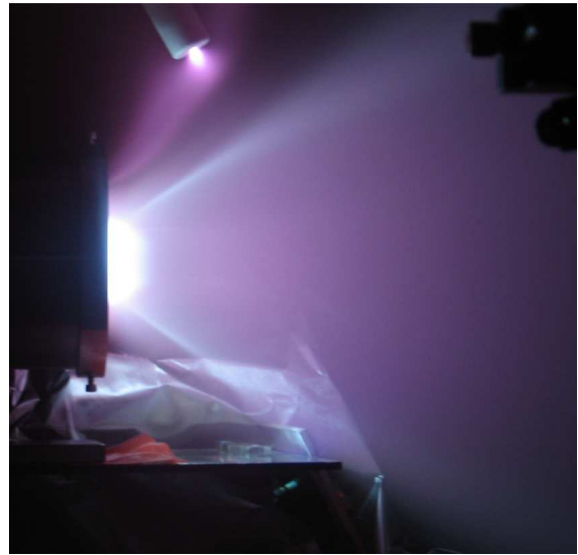
**Figure 7.** Anode current with varying anode potential at the flows indicated.

The scans performed with the thruster in this configuration revealed two modes of operation with a transition manifested by a sharp drop in both anode current and cathode keeper potential as the anode potential was increased. Visually, the discharge before the transition had a diffuse yet intense appearance while after the transition a bright, compact plume was visible near the thruster exit and a clear conical shell could be seen. Figure 8 shows photographs of the thruster operating in the two modes.

To reproduce the transition between modes, the potential scans were repeated several times at 7.0 and 10.0sccm with sufficient time allocated between trials for the thruster to cool down. It is evident in Fig. 7 that the transition point was recreated at approximately 450V to the anode during two independent scans at 10.0sccm, however; a third scan did not recreate the transition. In this case the anode current continued to rise with increasing anode potential. Similarly at 7.0sccm, the transition point shifted from approximately 300 to 410V between scans. At 8.0sccm no transition occurred and visual observations confirmed that the



(a) Visible discharge operating in the high anode current mode. Operating with 10 sccm of anode flow and 400 Volts applied to the anode.



(b) Visible discharge operating in the low anode current mode. Operating with 10 sccm of anode flow and 450 Volts applied to the anode.

**Figure 8. Two characteristic modes of operation of the DCHT**

thruster operated in the second, lower anode current and keeper potential, mode throughout the scan.

The connection between cathode keeper potential and mode transition is demonstrated in Fig. 9 for selected scans at 7.0 and 10.0sccm. Here both the anode current and keeper potential are seen to drop at the same applied anode potential. Although the keeper voltage and anode current drops are consistent, as anode potential was increased further the keeper potential began to increase while at 7.0sccm but remained low at 10.0sccm.

## B. Thrust Measurements at Busek

The thruster was taken to the Busek Company for thrust measurements. During these trials the cathode and anode positions were not changed from those during trials at SPL. Three scans at flow rates of 7.0, 8.5 and 10.0sccm were performed, see Fig. 10(a) for the anode currents measured during these trials. It was visually confirmed that the thruster operated in the lower current mode, appearing similar to Fig. 8(a), during the entire trial at 7.0sccm. At 8.5sccm a characteristic drop in anode current was observed at approximately 450V as the thruster transitioned to the low current mode. At 10.0sccm the thruster operated in the high current mode, visually similar to Fig. 8(b). During this final scan, the thruster was shut down after 400V was applied to the anode due to arcing observed between the thruster and cathode.

Thrust measurements taken at Busek are presented in Fig. 10(b). Thrust ranged from 6.0 to 16.0mN over all trials. During the apparent mode transition at 450V, while at 8.5sccm of anode flow, the thrust decreased sharply. Otherwise, the thrust was seen to increase with applied anode voltage. Thrust measurements along with the current data in Fig. 10(a) allowed for the anode thrust efficiency and specific impulse to be calculated using equations 1 and 2. The anode thrust efficiency is plotted in Fig. 10(d). The efficiency was

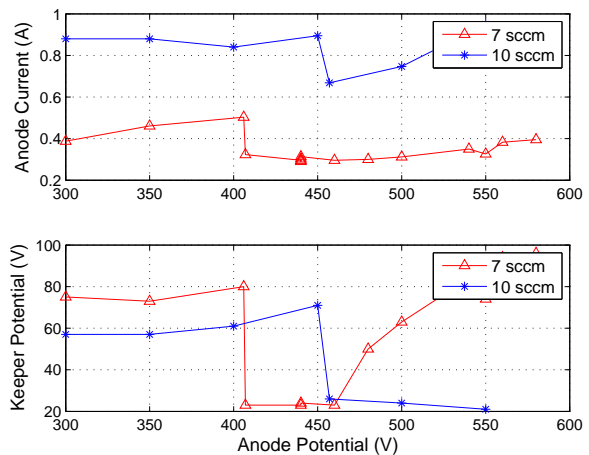


**Figure 9. Simultaneous drop in both anode current and cathode keeper potential during mode transition.**

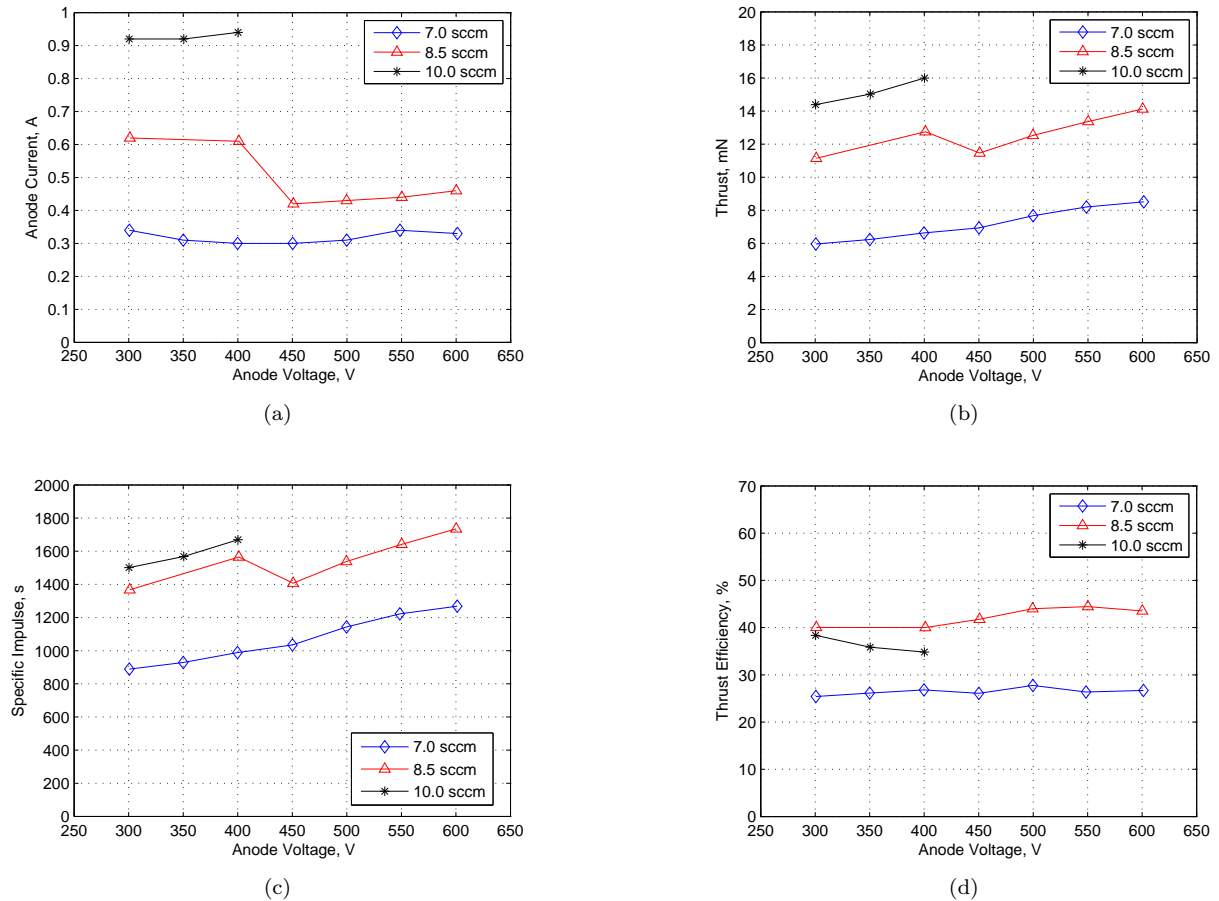


Figure 10. Anode current, thrust, anode thrust efficiency and specific impulse measurements taken at the Busek Company.

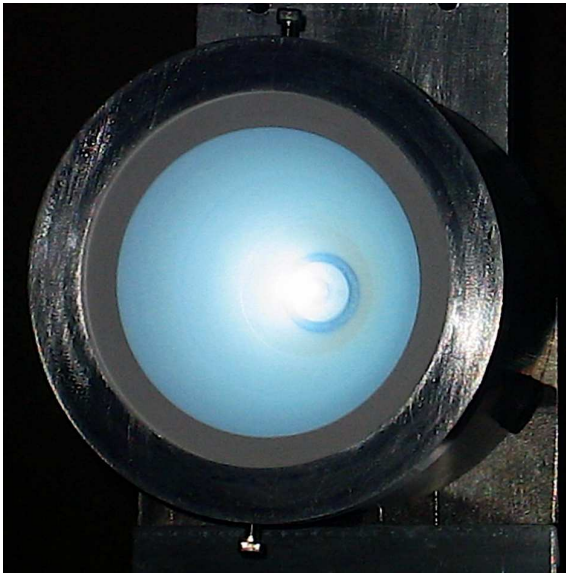
greatest during the 8.5sccm scan where it was over 40% at all times and had a maximum of 44.5% occurring with 550V applied to the anode. Here, a thrust of 13.4mN was measured while the DCHT consumed 242W of anode power. This was comparable to the Busek BHT-200, a more traditional Hall thruster, which at 200W provides 12.8mN of thrust at a propulsive efficiency of 43.5%.<sup>11</sup> The DCHT results are also comparable to the THALES DM7 thruster which had an anode efficiency of roughly 31%, delivering approximately 12mN of thrust with 10.0sccm of flow at 400V.<sup>3</sup>

Comparing the behavior of the thrust and anode thrust efficiency at 8.5sccm in Fig. 10 we observe that, despite a drop in thrust after the mode transition, the efficiency increased slightly. This suggests that the second mode may be, overall, a more efficient state. The specific impulse is plotted in Fig. 10(c). With the exception of the mode transition at 8.5sccm the  $I_{sp}$  increased at a rate comparable to the expected square root dependence on anode voltage.

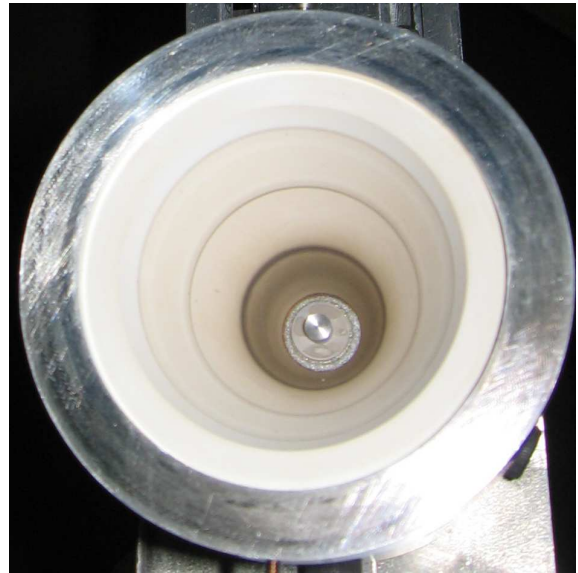
### C. Physical Observations

Figure 11(b) is a photograph of the DCHT conical discharge channel after approximately 2 hours of total firing time (comprised of several short trials lasting no more than 25 minutes each). Distinct dark bands are visible at each cusp. The amount of deposition transitions sharply at the cusps, with the most deposition closest to the anode. The ceramic cone was easily cleaned at this stage suggesting that the discolouration was due to sputtered deposition only, with no erosion or pitting observed. Darkness due to deposition suggests a lack of high energy ions striking those surfaces. These observations are consistent with the predicted benefits of using cusped fields to create magnetic mirrors for plasma containment.

Figure 11(a) shows the brightest region of the thruster plasma localized away from the ceramic walls.



(a) Photograph of discharge showing brightest regions of plasma separated from channel walls.



(b) Boron Nitride cone after approximately 2 hours of firing. The three darkest rings coincide with the magnet boundaries.

**Figure 11. Visual observations of the DCHT discharge.**

This further suggests that the cusped fields are protecting the surface, as desired. The effectiveness of the magnetic bottle near the anode localizing the plasma away from the anode tip is inconclusive at this stage. Although Fig. 11(b) shows the anode in good condition, the ceramic washer above the propellant inlet was damaged. This was likely due to a combination of ion sputtering and arcing during early stages of testing. However; further tests after repairing the damaged washer resulted in no damage or deposition on the washer but significant deposition on the anode tip itself.

#### **D. Future Work**

Further testing of the DCHT will be performed over a greater range of flow rates and anode potentials. In addition, the transition between modes will be examined in closer detail in an effort to fully characterize the phenomenon. Furthermore, the thruster characterization will continue with both RPA and Faraday cup measurements of the thruster plume. Finally, both the anode position and cathode location will be varied systematically in order to quantify their impacts on performance and determine an optimal arrangement.

## **VI. Conclusion**

An experimental thruster using cusped magnetic fields and featuring a divergent discharge channel has been constructed and successfully tested. Initial trials, performed at the MIT SPL and the Busek Company, have revealed promising results regarding the ability of cusped field thrusters to contain a discharge plasma while performing at levels comparable to traditional Hall thrusters. During operation, two distinct modes of operation were observed. The transition between modes was observed to consist of a drop in anode current and thrust along with a visual change in the thruster plume. Observations of the thruster after firing revealed a clear pattern of deposition along the channel walls with the greatest deposition occurring at the magnetic cusps. Finally, the position of the neutralizing cathode appeared to have a significant impact on the thruster operating characteristics suggesting that an optimal position may exist.

## Acknowledgments

The hollow cathode and testing facilities volunteered to us by the Busek Company of Natick, MA were invaluable to this project. Specifically the authors would like to thank Michael Tsay for overseeing testing at Busek. Finally we would like to thank Professor Paulo Lozano for his contributions to the thruster design.

## References

- <sup>1</sup>Raitses, Y. and Fisch, N. J., "Parametric Investigations of a Nonconventional Hall Thruster," *Physics of Plasmas*, Vol. 8, No. 5, 2001.
- <sup>2</sup>Kornfeld, G., Koch, N., and Coustou, G., "First Test Results of the HEMP Thruster Concept," *28<sup>th</sup> International Electric Propulsion Conference*, Toulouse, France, March 2003, also IEPC-03-134.
- <sup>3</sup>Kornfeld, G., Koch, N., and Harmann, H. P., "New Performance and Reliability Results of the THALES HEMP Thruster," *4<sup>th</sup> International Spacecraft Propulsion Conference*, Cagliari, Italy, June 2004.
- <sup>4</sup>Koch, N., Harmann, H. P., and Kornfeld, G., "Development and Test Status of the THALES High Efficiency Multi-stage Plasma (HEMP) Thruster Family," *29<sup>th</sup> International Electric Propulsion Conference*, Princeton University, October-November 2005.
- <sup>5</sup>Kornfeld, G., "Plasma Accelerator Arrangement," United States Patent 6,523,338 B1, 2003.
- <sup>6</sup>Sovey, J. S., "Improved Ion Containment Using a Ring-Cusp Ion Thruster," *16<sup>th</sup> International Electric Propulsion Conference*, New Orleans, LA, November 1982, also AIAA-82-1928.
- <sup>7</sup>Warner, N. Z. and Martinez-Sanchez, M., "Design and Preliminary Testing of a Miniaturized TAL Hall Thruster," *39<sup>th</sup> Joint Propulsion Conference and Exhibit*, Sacramento, CA, July 2006, also AIAA-2006-4994.
- <sup>8</sup>Technologies, D. M., "Somarium Cobalt (Sm-Co) Magnets," <http://www.dextermag.com/Samarium-Cobalt.aspx>.
- <sup>9</sup>SAINT GOBAIN BORON NITRIDE, [www.bn.saint-gobain.com/](http://www.bn.saint-gobain.com/).
- <sup>10</sup>Cheng, S. Y.-M., "Modeling of Hall Thruster Lifetime and Erosion Mechanisms," Ph.D. Thesis, Massachusetts Institute of Technology, Cambridge, MA, *in preparation*.
- <sup>11</sup>BUSEK CO., "[www.busek.com](http://www.busek.com)," .